P H Y S I C A L R E V I E W L E T T E R S

Spin Squeezing of Atomic Ensembles via Nuclear-Electronic Spin Entanglement

T. Fernholz, H. Krauter, K. Jensen, J. F. Sherson,* A. S. Sørensen, and E. S. Polzik[†]

*QUANTOP, Danish National Research Foundation Center for Quantum Optics, Niels Bohr Institute, Copenhagen University,
DK 2100, Denmark*

We demonstrate spin squeezing in a room temperature ensemble of $\approx 10^{12}$ cesium atoms using their internal structure, where the necessary entanglement is created between nuclear and electronic spins of each individual atom. This state provides improvement in measurement sensitivity beyond the standard quantum limit for quantum memory experiments and applications in quantum metrology and is thus a complementary alternative to spin squeezing obtained via interatom entanglement. Squeezing of the collective spin is verified by quantum state tomography.

Entangled many body systems have recently attracted significant attention in various contexts. Among them, spin squeezed atoms and ions have raised interest in the field of precision measurements, as they allow one to overcome quantum noise of uncorrelated particles [1–5]. Precise quantum state engineering is also required as a resource for quantum computation, and spin squeezing can be used to create multipartite entangled states [6]. Two-mode squeezing has served for the creation of entanglement between macroscopic objects, i.e., ensembles of neutral atoms [7], which have emerged as important systems for the storage of quantum information [8–16]. It has been shown that ensemble spin squeezing can be used to significantly improve the fidelity of some existing quantum memory protocols [8]. In the majority of the work on ensemble entanglement, alkali atoms used as memory units were treated as spin-1/2 systems, while their actual total angular momenta were considered an unfortunate complication. Entanglement in those experiments could therefore be generated only between different atoms of the ensemble [17,18]. In this Letter, we demonstrate for the first time ensemble spin squeezing in a room temperature ensemble of $\approx 10^{12}$ spin-4 atoms by using their internal structure to squeeze the individual spins. Indeed, we can show that spin squeezing within the cesium $F = 4$ manifold is a signature of entanglement between the electron and the nucleus. However, as discussed below, the ensemble spin squeezing does not necessarily follow from the single atom spin squeezing. Therefore, we verify the collective squeezing by measurement of the collective spin state via strong coupling to off-resonant light. In particular, we perform for the first time quantum tomography of a nonclassical state of an atomic ensemble.

We first consider a collection of electronic ground state atoms ($L = 0$), each prepared in the magnetic sublevel $|F = 4, m_F = 4\rangle$ with respect to the x quantization axis. This fully stretched state is a product state, where both the nuclear and the electronic spin are in eigenstates of their angular momentum projection operators with maximal eigenvalues $I_x = 7/2$ and $S_x = 1/2$, respectively. In the following, we denote the total spin operator of the en-

semble $\hat{\mathbf{J}}$. For large atom numbers N, the total spin becomes macroscopic with $\langle\hat{\mathbf{J}}\rangle = (J, 0, 0)$ in Cartesian coordinates, and $J = \hbar N F$. The commutation relation $[\hat{J}_y, \hat{J}_z] = i\hbar\hat{J}_x$ imposes an uncertainty relation, and the fully pumped ensemble is in a minimal uncertainty state with $(\Delta\hat{J}_y)^2 = (\Delta\hat{J}_z)^2 = \hbar J/2$. Such states are called coherent spin states (CSS) and set the standard quantum limit (SQL) to spin projection measurements. For a squeezed spin state, one of the orthogonal projections exhibits an uncertainty below the SQL. For useful spin squeezing, however, it is not sufficient to reduce the uncertainty below its initial value [$\chi^2 = 2(\Delta\hat{J}_\perp)^2/\hbar J < 1$], but to compare it to a CSS with the same mean spin [$\zeta^2 = 2(\Delta\hat{J}_\perp)^2/\hbar\langle|\hat{\mathbf{J}}|\rangle < 1$] [1,19], or even more rigorously to the initial uncertainty in spin angle [$\xi^2 = 2J(\Delta\hat{J}_\perp)^2/\hbar\langle|\hat{\mathbf{J}}|\rangle^2 < 1$] [20,21]. The last condition is the strongest and necessarily requires entanglement of elementary spin-1/2 constituents [22]. This condition, which has to be met to improve quantum metrology, e.g., the precision of atomic clocks with a given number of atoms, is fulfilled in the present work.

Spin squeezing can be achieved by applying an interaction that depends nonlinearly on Cartesian spin components orthogonal to the mean spin [19]. A Hamiltonian of the form $\hat{H}_s = \alpha\hat{F}_z^2$ acting on a spin $\hat{\mathbf{F}}$ induces a process called one-axis twisting. Starting from a CSS aligned along the x direction, the spin is rotated about the z axis in proportion to its fluctuating z component. The initially symmetric quasiprobability distribution (QPD) will be sheared and appear squeezed in the y, z plane in a slightly rotated basis $\hat{F}_{y'}, \hat{F}_{z'}$. At the same time, the mean spin is reduced as the QPD bends around the spherical phase space for constant F.

We generate such squeezing Hamiltonian using the tensor light shift induced by an off-resonant light field. In case of linear polarization along the z direction with classical field amplitude E_z, the interaction with an atomic spin $\hat{\mathbf{F}}$ reduces to an atomic Hamiltonian of the form [23]:

$$H_s = -\tfrac{1}{4}(\alpha_0|E_z|^2 + \alpha_2|E_z|^2\hat{F}_z^2). \qquad (1)$$

While the scalar polarizability α_0 simply results in an overall Stark shift, its tensor part, proportional to α_2, provides the basis for spin squeezing.

In the x basis, the z-polarized field can be decomposed into equally strong σ_+ and σ_- components, driving Raman transitions between magnetic sublevels ($\Delta m = 2$). With a magnetic field along the x direction, the above description remains valid after transformation to a frame corotating with the Larmor frequency ω_L. Consequently, the frequencies of the two Raman fields have to be shifted by $\pm\omega_L$ to meet the two-photon resonance condition [see Fig. 1(b)]. In this sense, spin squeezing corresponds to the creation of paired excitations of the spin at frequency $2\omega_L$ and will reveal itself in the Fourier component of the rotating spin at frequency ω_L.

Naturally, this type of interaction is nonlinear only in spin components of individual atoms. Therefore, the maximally possible degree of squeezing [6] is limited by the total spin of a single atom, while the total spin of an ensemble can be arbitrarily high. With one-axis twisting, the squeezing is further limited by the deviation of the resulting QPD from a geodesic in the spherical phase space. This finding is equivalent to the differential light shift imposed on magnetic sublevels in the x basis, which
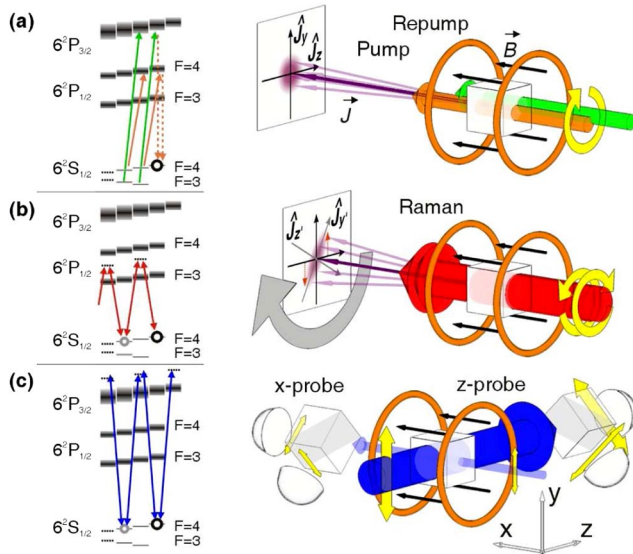

FIG. 1 (color online).   Pulse sequence and level scheme for atomic state preparation and quantum state reconstruction. (a) Optical pumping creates a macroscopic spin $\vec{J}$ in a CSS, aligned with the magnetic field $\vec{B}$ in the x direction. (b) A Raman transition creates a coherent superposition of even magnetic sublevels, which shears the QPD in the rotating frame and decreases the mean spin. (c) The spin state of the ensemble is characterized via off-resonant Faraday interaction with a linearly polarized probe beam, propagating in the z direction. Quantum noise limited polarization measurements in a 45° basis reveal the statistics of the atomic angular momentum projections $\hat{J}_{y'}$ and $\hat{J}_{z'}$, which are precessing about the x axis. Simultaneously, a weak measurement along the x axis determines the magnitude of the mean atomic spin $\langle \hat{J}_x \rangle$.

inevitably accompanies the Raman coupling and detunes the coupling between different sublevels. A somewhat higher degree of squeezing can be achieved with a two-axis countertwisting Hamiltonian of the form $H_s = \alpha(\hat{F}_z^2 - \hat{F}_y^2)$ [19]. Taking the decreasing mean spin into account, squeezing parameters of $\chi^2 \approx 0.163$, $\zeta^2 \approx 0.247$, and $\xi^2 \approx 0.327$ can be reached with this Hamiltonian, using the maximum available spin of $F = 4$ in ground state cesium atoms. The required Hamiltonian could, e.g., be implemented with two laser fields of orthogonal polarizations (along rotating y' and z' directions) and opposite detunings from an atomic resonance. Here, we balance the light shift instead with the second-order Zeeman shift $\hat{H}_Z = \beta\hat{F}_x^2$, such that all energy splittings between magnetic substates of the $F = 4$ manifold coincide. By adjusting the light intensity and detuning, $\alpha_2|E_z|^2 = -8\beta$ can be chosen to obtain $\hat{H}_s + \hat{H}_Z = -\frac{\alpha_0|E_z|^2}{4} + \beta\hbar^2 F(F+1)/2 + \beta(\hat{F}_z^2 - \hat{F}_y^2)/2$, using $\hat{F}_x^2 + \hat{F}_y^2 + \hat{F}_z^2 = \hbar^2 F(F+1)$ for eigenstates of $\hat{\mathbf{F}}^2$.

Coherent superpositions of magnetic sublevels similar to those described above have been recently generated by universal quantum control of a hyperfine spin in an ultracold ensemble [24] in the weak coupling limit. In that experiment the average single atom density matrix was determined. However, knowledge of the single atom density matrix is not sufficient to infer spin squeezing of the ensemble. Because of the collective preparation, the members of the ensemble will not in general be uncorrelated. Collective spin squeezing, as required for quantum limited metrology or quantum memory [7], can therefore only be determined via measurement of collective quantum fluctuations, ideally via full quantum tomography, as performed in the present Letter. Only such measurements can reveal the deleterious effect of classical and quantum atom-atom correlations, which can be created in the preparation process and can easily ruin the spin squeezing of the ensemble. In particular, it is of major importance to send the driving Raman field [Fig. 1(b)] along the direction of the mean spin (x direction). If, e.g., the orthogonal y direction is used, the quantum fluctuations of the driving field will couple via atomic π transitions to the collective symmetric mode for $\Delta m_x = 1$ coherences, and thus destroy collective spin squeezing under strong coupling conditions. In fact, this process forms the basis for quantum memory applications [8,9].

In our experiment, we employ a room temperature ensemble of $N \approx 10^{12}$ ^{133}Cs atoms, contained in a paraffin coated $22 \times 22 \times 22$ mm^3 glass cell. The cell is shielded against field fluctuations and subjected to a homogeneous magnetic field along the x direction of $B_x \approx 0.9$ G. By fine tuning the magnetic field we adjust the atomic Larmor precession to a reference frame rotating at $\omega_L = 2\pi \times 322$ kHz, which is defined by a computer controlled radio frequency (rf) synthesizer.

The experimental pulse sequence consists of three stages and is depicted in Fig. 1. The two-step state preparation

starts with an 8 ms long optical pump pulse of two reso-
nant, circularly polarized beams, propagating along the
x direction. See Fig. 1(a). After optical pumping, we find
98% of the atoms in the $|F = 4, m_x = 4\rangle$ state, by evaluat-
ing the magneto-optical resonance signal (MORS) [25]. At
the second stage, we coherently transfer atomic population
between even magnetic substates of the $F = 4$ manifold by
driving Raman transitions on the D_1-line for a variable
duration $T_R = 0$–6 ms with a single photon detuning of
$\Delta_R = -550$ MHz from the $6^2S_{1/2}, F = 4 \rightarrow 6^2P_{1/2}, F' =$
4 transition. See Fig. 1(b). The two-photon difference
$\nu_R \approx 644.2$ kHz is resonant with the $m_x = 4 \rightarrow m_x = 2$
transition, including corrections for second-order Zeeman
and differential light shifts. Finally, the collective atomic
state is analyzed via off-resonant Faraday interaction with
a strong ($P \approx 5$ mW), linearly polarized, 2 ms long probe
pulse. The probe laser frequency is close to the D_2 line with
a blue detuning of $\Delta_P = 825$ MHz from the $F = 4 \rightarrow$
$F' = 5$ transition. See Fig. 1(c).

Some experimental issues have to be considered for the
generation of collective squeezed states. The state prepa-
ration must be completed on a time scale short compared to
decoherence mechanisms, e.g., caused by inhomogeneous
fields, atom-atom, and atom-wall collisions. Therefore, the
strength of the squeezing interaction should be maximized.
Although atomic motion leads to averaging, it is necessary,
particularly on short time scales, to provide rather homo-
geneous coupling strength over the cell volume with ex-
panded, mode-matched Raman fields. A small angle
between the two beams leads to a varying relative phase
over the cell volume, which gives rise to a residual Doppler
shift for moving atoms and results in incoherent squeezing.
A similar effect is caused by the collective spin of the
polarized ensemble. Because of the Faraday effect, the
sample is circularly birefringent and induces a phase shift
over the cell length, $\Delta\phi < 12°$ for our parameters. A
simple and robust experimental approach is to generate
the necessary Raman fields by amplitude modulation of a
single, linearly polarized light beam. But to avoid the
additional sidebands and minimize spontaneous emission,
we mode-match two phase-stable, circularly polarized
fields. For ground state alkali atoms, the tensor polariz-
ability compared to the scattering rate is limited by the
excited state hyperfine splitting. Their ratio is optimal
when tuned between the hyperfine transitions of the D_1
line, ($F = 4 \rightarrow F' = 3, 4$) at 894 nm for cesium. At this
detuning, the tensor polarizability is also largest and sta-
tionary and thus independent of atomic velocity. In addi-
tion, it has the correct sign for compensation of the second-
order Zeeman shift.

The protocol for atomic quantum tomography which we
use to reconstruct the collective quantum state is detailed
elsewhere [9,23,26]. In brief, we send a strong, linearly
y-polarized beam along the z axis of the atomic ensemble,
see Fig. 1(c). After the interaction with duration T, we
perform polarization homodyning in the 45° basis, mea-

suring the photon number difference in the two outputs,
i.e., the Stokes operator $\hat{S}_y = \hat{n}_{+45°} - \hat{n}_{-45°}$. It is conve-
nient to express this operator and its conjugate in the
canonical form as $\hat{y} = \hat{S}_y/\sqrt{\langle\hat{S}_x\rangle}$, $\hat{q} = \hat{S}_z/\sqrt{\langle\hat{S}_x\rangle}$ for light
variables of a given mode with $[\hat{y}, \hat{q}] \approx i$. Because of the
Faraday effect, the polarization of the input beam is rotated
proportionally to the instantaneous atomic spin component
$\hat{J}_z$, producing a proportional homodyne output for small
rotations. The atomic spin precesses, and information on
the two orthogonal, rotating spin components $\hat{J}_{y'}$ and $\hat{J}_{z'}$
can be obtained by evaluating the cosine and sine compo-
nents of the output signal at the Larmor precession fre-
quency ω_L. The spin operators in the canonical form are
$\hat{x} = \hat{J}_{y'}/\sqrt{\hbar\langle\hat{J}_x\rangle}$, $\hat{p} = \hat{J}_{z'}/\sqrt{\hbar\langle\hat{J}_x\rangle}$.

The atomic ensemble is freshly prepared and the proce-
dure repeated 10^4 times to determine the quantum statistics
including the mean and variance of the collective atomic
spin state. The statistical moments of the spin components
can be inferred from the moments of the probe light output
as shown in [9]:

$$(\Delta\hat{y}_{0,\text{out}}^{c,s})^2 = (\Delta\hat{y}_0^{c,s})^2 + \frac{\kappa^2}{2}(\Delta\hat{x}, \Delta\hat{p})^2 + \frac{\kappa^4}{12}(\Delta\hat{q}_1^{s,c})^2. \quad (2)$$

The first term is the shot noise of the light probe, the second
term presents the spin variances we wish to measure, and
the third term is an extra vacuum noise contribution from
the quantum back action of the measurement [9]. The
indices correspond to different, nonorthogonal temporal
modes of the light field, oscillating as cosine (c) and sine
(s) components at the Larmor frequency.

We scale the time-integrated homodyne output by refer-
encing it to the light vacuum noise, $\langle(\Delta\hat{y})^2\rangle = \langle(\Delta\hat{q})^2\rangle =$
$1/2$. The coupling strength $\kappa^2 \propto J_x T$ is calibrated by mea-
suring the noise of the atomic ensemble spin in thermal
equilibrium (unpolarized spin state). For the thermal state,
the measurement back-action noise is zero and the output
noise is given by the light noise and the atomic contribu-
tions from thermally populated states in the $F =$
4 manifold: $(\Delta\hat{y}_{0,\text{out}}^{c,s})^2 = \frac{1}{2} + \frac{\kappa^2}{2\hbar J_x}(\Delta\hat{J}_{y',z'})^2 = \frac{1}{2} + \frac{\kappa^2 N\hbar}{2J_x}\frac{15}{16}$.
In principle, the second-order Zeeman splitting has to be
considered, but it is compensated by the differential light
shift induced by the probe laser. The measurement of the
mean spin J_x/N is calibrated with a fully pumped
ensemble.

The state tomography is illustrated in Fig. 2. Atomic
variances are directly inferred from the sampled data. In
addition, we performed maximum likelihood estimations
of the collective state in the 10 best-resolved dimensions of
Hilbert space [27]. The shown density matrix is repre-
sented in the Fock state basis given by the excitation
operators b, $b^\dagger = (\hat{x} \pm i\hat{p})/\sqrt{2}$ and $\hat{m}, \hat{n} = b^\dagger b$.

The results, i.e., the measured variances, are shown in
Fig. 3 together with predictions from a single atom density
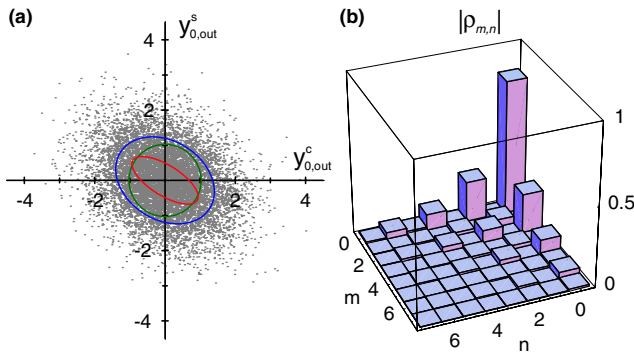matrix calculation. Our model includes atomic decay due

(a)

(b)

FIG. 2 (color online).   Exemplified quantum state reconstruction (at ≈ 3 dB squeezing) with $\kappa^2 \approx 0.8$. (a) Scatter plot of 10^4 realizations. The atomic covariance (inner ellipse with $\sqrt{2}\sigma$ radii) is determined by correcting the total covariance (outer ellipse) for light and back-action noise (circle). (b) Maximum likelihood estimation of the density matrix $\hat{\rho}$ for the collective spin state, showing alternating excitation numbers m, n in the harmonic oscillator approximation.

to spontaneous emission and incorporates independently measured values for depolarizing and dephasing times in the dark ($T_1 = 80$ ms, $T_2 = 20$ ms). We kept the effective light power in the cell as a free model parameter, but especially for short times, the theoretical results are stable against small variations in the control parameters. The used light power slightly overcompensates the second-order Zeeman shift, and our model suggests better performance at even higher powers as it identifies atomic decay as the dominant limitation. We consistently achieve squeezing of a canonical variable by $\zeta^2 = 0.47 \pm 0.1$. Quantum memory [8] and metrology applications gain by an increased signal-to-noise ratio of approximately 3 dB as $\xi^2 = 0.54 \pm 0.1$.

In conclusion, we demonstrated squeezing of a collective spin with a noise reduction of ≈ -3 dB by generation of entanglement within individual members of the en-
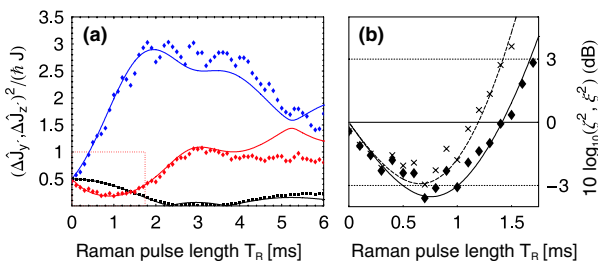

FIG. 3 (color online).   (a) Results of the quantum state reconstruction for varied pulse length. Shown are atomic squeezed ($\equiv \chi^2/2$) and antisqueezed variances (diamonds). For useful squeezing, they have to be compared to the variance of a CSS with the same mean spin (squares). (b) Resulting squeezing parameters ζ^2 (diamonds) and ξ^2 (crosses) in decibels, representing renormalized data from the indicated region in (a). Theoretical predictions are shown as solid and dashed lines.

semble. We have fully characterized the nonclassical collective atomic state via quantum state tomography. The demonstrated method is independent and complementary to the ensemble entanglement and squeezing approach based on quantum-nondemolition (QND) measurements [7,18]. Indeed it can, e.g., be directly applied, either separately or in combination with the QND method, to enhance the fidelity of the quantum memory [8]. It may also find use in spectroscopic applications, such as magnetometry beyond the SQL.

*Present address: Institut für Physik, Johannes-Gutenberg Universität, D-55099 Mainz, Germany.
†polzik@nbi.dk

[1] M. Kitagawa and M. Ueda, Phys. Rev. Lett. **67**, 1852 (1991).
[2] D. Leibfried *et al.*, Science **304**, 1476 (2004).
[3] V. Petersen, L. B. Madsen, and K. Mølmer, Phys. Rev. A **71**, 012312 (2005).
[4] C. F. Roos *et al.*, Nature (London) **443**, 316 (2006).
[5] P. J. Windpassinger *et al.*, Phys. Rev. Lett. **100**, 103601 (2008).
[6] A. S. Sørensen and K. Mølmer, Phys. Rev. Lett. **86**, 4431 (2001).
[7] B. Julsgaard, A. Kozhekin, and E. S. Polzik, Nature (London) **413**, 400 (2001).
[8] B. Julsgaard *et al.*, Nature (London) **432**, 482 (2004).
[9] J. F. Sherson *et al.*, Nature (London) **443**, 557 (2006).
[10] L.-M. Duan, M. D. Lukin, J. I. Cirac, and P. Zoller, Nature (London) **414**, 413 (2001).
[11] D. Matsukevich *et al.*, Phys. Rev. Lett. **96**, 030405 (2006).
[12] C.-W. Chou *et al.*, Science **316**, 1316 (2007).
[13] S. Chen *et al.*, Phys. Rev. Lett. **99**, 180505 (2007).
[14] J. Simon *et al.*, Phys. Rev. Lett. **98**, 183601 (2007).
[15] K. Honda *et al.*, Phys. Rev. Lett. **100**, 093601 (2008).
[16] J. Appel *et al.*, Phys. Rev. Lett. **100**, 093602 (2008).
[17] J. Hald *et al.*, Phys. Rev. Lett. **83**, 1319 (1999).
[18] A. Kuzmich, L. Mandel, and N. P. Bigelow, Phys. Rev. Lett. **85**, 1594 (2000).
[19] M. Kitagawa and M. Ueda, Phys. Rev. A **47**, 5138 (1993).
[20] D. J. Wineland *et al.*, Phys. Rev. A **46**, R6797 (1992).
[21] D. J. Wineland, J. J. Bollinger, W. M. Itano, and D. J. Heinzen, Phys. Rev. A **50**, 67 (1994).
[22] A. Sørensen *et al.*, Nature (London) **409**, 63 (2001).
[23] J. Sherson, B. Julsgaard, and E. S. Polzik, Adv. At. Mol. Opt. Phys. **54**, 81 (2006).
[24] S. Chaudhury *et al.*, Phys. Rev. Lett. **99**, 163002 (2007).
[25] B. Julsgaard, J. Sherson, J. L. Sørensen, and E. S. Polzik, J. Opt. B **6**, 5 (2004).
[26] K. Usami, J.-i. Takahashi, and M. Kozuma, Phys. Rev. A **74**, 043815 (2006).
[27] Z. Hradil, D. Mogilevtsev, and J. Řeháček, Phys. Rev. Lett. **96**, 230401 (2006).